Werk

Terms and Conditions

Contact

Niedersächsische Staats- und Universitätsbibliothek Göttingen
Georg-August-Universität Göttingen
Platz der Göttinger Sieben 1
37073 Göttingen
Germany
Email: gdz@sub.uni-goettingen.de

J Geophys (1987) 61:190–199

Journal of Geophysics

Canonical decomposition of the telluric transfer tensor

E. Yee and K.V. Paulson
Cybernetics Laboratory, Department of Physics, University of Saskatchewan, Saskatoon S7N0W0, Canada

Abstract. This paper presents an analysis of the telluric transfer tensor **T** based on canonical decomposition, which explicitly displays the structural components of the tensor in the form of eight physically motivated scalar parameters and, hence, provides a complete specification of the information embodied in **T**. These canonical telluric parameters provide the proper framework for the interpretation, identification and discrimination of the geoelectric contributions to the telluric response from all the various dimensional conductivity structures. For a strictly two-dimensional (2-D) geoelectric structure, only five of the canonical parameters are relevant and this fact provides the motivation for the development of a procedure for the separation of the 2-D and 3-D structural contribution to **T**. This separation procedure consists of two steps: firstly, a normal telluric tensor $\mathbf{T}_N$ is extracted from **T** based on the optimization of an appropriate cost function; and secondly, the complex input (or output) principal coordinate frame for $\mathbf{T}_N$ is computed by canonical decomposition and a real coordinate frame consisting of linearly polarized basis states is chosen so as to approximate this principal complex frame in an optimum fashion. Finally, the canonical decomposition of the magnetic transfer matrix is derived and its utilization for the identification of the geoelectric strike and dip directions for near 2-D structures is considered.

Key words: Telluric mapping method – Telluric transfer tensor – Canonical decomposition – Magnetic transfer matrix – Induction vector – Structural dimensionality

Introduction

The telluric mapping method (Yungul, 1966) is based on the relationship between the tangential components of the natural electric field measured simultaneously at two separated locations on the surface of the earth. Two transverse (1, 2) and (1′, 2′) Cartesian coordinate systems are chosen at the fixed base station (O) and the roving satellite station (O') for the measurement of the electric field. We will use the standard Dirac bra-ket notation whereby the vectors of a Hilbert space over the complex numbers are denoted by kets, $|a\rangle$, and the vectors of the dual space by bras, $\langle b|$. To make the connection with the usual vector notation, we note that the components of the ket $|a\rangle$ in some chosen representation can be arranged into some column vector **a**, whereas the components of the corresponding bra $\langle a|$ in the same representation can be arranged into a row vector $\mathbf{a}^\dagger$, where † denotes Hermitian transposition. In this notation, the bra-ket product $\langle a|b\rangle$ can be expressed as the scalar product of the row vector $\mathbf{a}^\dagger$ and the column vector **b** corresponding to $\langle a|$ and $|b\rangle$, respectively, so $\langle a|b\rangle = \mathbf{a}^\dagger \cdot \mathbf{b} = \sum_i a_i^* b_i$, where a_i and b_i denote the (complex) components of **a** and **b** and $*$ denotes complex conjugation. Now, for a vertically incident monochromatic plane-wave source field, the coupling between the transverse electric fields observed at O and O' can be represented by the following linear relationship (cf. Fig. 1):

$$|E^s_{1',2'}\rangle \equiv \begin{pmatrix} E^s_{1'} \\ E^s_{2'} \end{pmatrix} = \begin{pmatrix} T_{1'1} & T_{1'2} \\ T_{2'1} & T_{2'2} \end{pmatrix} \begin{pmatrix} E^b_1 \\ E^b_2 \end{pmatrix} \equiv \mathbf{T}|E^b_{1,2}\rangle, \tag{1}$$

where $|E^b_{1,2}\rangle$ and $|E^s_{1',2'}\rangle$ are the base and satellite ket vectors, respectively, whose elements (phasor components) are the complex electric field amplitudes measured with respect to the sensor coordinate systems (1, 2) and (1′, 2′). Here, **T** is the telluric transfer tensor which characterizes the transfer properties of the earth system coupling the O to O' channel. For the assumed source (primary) field, the elements of the telluric transfer tensor depend upon the electrical conductivity characterizing the internal structure of the earth system, the coordinate systems used to measure the electric fields at the base and satellite stations (which need not be the same), the frequency at which the measurements were made and the relative positions of the base and satellite stations on the earth's surface.

The telluric transfer matrix **T** can be expressed in terms of the identity matrix and the three Pauli spin matrices as follows:

$$\mathbf{T} = \sum_{\nu=0}^{3} T_\nu \Upsilon_\nu, \tag{2}$$

where

$$\Upsilon_0 = \mathbf{I} = \begin{pmatrix} 1 & 0 \\ 0 & 1 \end{pmatrix},$$

$$\Upsilon_1 = \begin{pmatrix} 0 & 1 \\ 1 & 0 \end{pmatrix},$$

$$\Upsilon_2 = \begin{pmatrix} 0 & -i \\ i & 0 \end{pmatrix},$$

Offprint requests to: K.V. Paulson

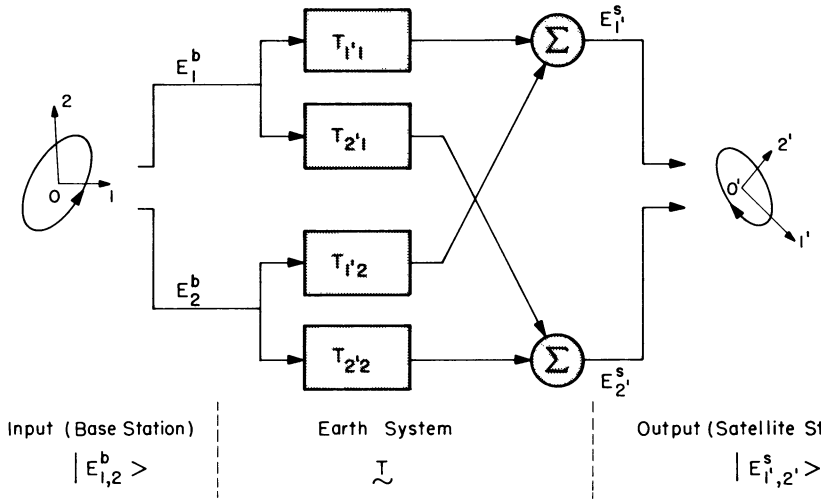

Fig. 1. The relevant components of the telluric mapping method. $|E^b_{1,2}\rangle$ and $|E^s_{1',2'}\rangle$ are the base (input) and satellite (output) electric field ket vectors (vector phasors) sensed with reference to the transverse Cartesian coordinate systems (1, 2) and (1′, 2′) at points O (fixed base station) and O' (roving satellite station). These vector phasors are linearly related through the telluric transfer tensor $\mathbf{T}$ which characterizes the transfer properties of the earth system

and

$$\Upsilon_3=\begin{pmatrix}1 & 0\\ 0 & -1\end{pmatrix}.$$

Since these basis matrices are trace-orthogonal [i.e. $tr(\Upsilon_\mu \Upsilon_\nu)=2\delta_{\mu\nu}$ where $\delta_{\mu\nu}$ denotes the Kronecker delta function], the expansion coefficients of Eq. (2) may be computed as $T_\nu=tr(\mathbf{T}\Upsilon_\nu)/2$ ($\nu=0, 1, 2, 3$); more explicitly, these coefficients are given by

$$T_0=(T_{1'1}+T_{2'2})/2, \tag{3a}$$
$$T_1=(T_{1'2}+T_{2'1})/2, \tag{3b}$$
$$T_2=i(T_{1'2}-T_{2'1})/2, \tag{3c}$$

and

$$T_3=(T_{1'1}-T_{2'2})/2. \tag{3d}$$

We note that T_0 and T_2 are rotationally invariant parameters, viz. they are invariant under the rotation transformation of $\mathbf{T}$

$$\mathbf{T}'(\psi)\equiv\begin{pmatrix}T'_{1'1}(\psi) & T'_{1'2}(\psi)\\ T'_{2'1}(\psi) & T'_{2'2}(\psi)\end{pmatrix}=\mathbf{R}(\psi)\,\mathbf{T}\mathbf{R}(-\psi), \tag{4a}$$

where

$$\mathbf{R}(\psi)=\cos\psi\ \Upsilon_0+i\sin\psi\ \Upsilon_2=\begin{pmatrix}\cos\psi & \sin\psi\\ -\sin\psi & \cos\psi\end{pmatrix} \tag{4b}$$

is the rotation matrix associated with a counter-clockwise rotation through angle ψ about the vertical z-axis. Similarly, T_0 and T_1 are ellipticity invariant parameters, viz. they are invariant under the ellipticity transformation of $\mathbf{T}$

$$\bar{\mathbf{T}}(\lambda)\equiv\begin{pmatrix}\bar{T}_{1'1}(\lambda) & \bar{T}_{1'2}(\lambda)\\ \bar{T}_{2'1}(\lambda) & \bar{T}_{2'2}(\lambda)\end{pmatrix}=\mathbf{P}(-\lambda)\,\mathbf{T}\mathbf{P}(\lambda), \tag{5a}$$

where

$$\mathbf{P}(\lambda)=\cos\lambda\ \Upsilon_0+i\sin\lambda\ \Upsilon_1=\begin{pmatrix}\cos\lambda & i\sin\lambda\\ i\sin\lambda & \cos\lambda\end{pmatrix} \tag{5b}$$

is the ellipticity matrix for angle $\lambda(\lambda\in[-\pi/4, \pi/4])$. The physical significance of rotation and ellipticity transformations, particularly as it would relate to the polarization characteristics of the base (input) and satellite (output) electric fields, is discussed in greater detail in Yee and Paulson (1987).

It is important to be able to relate the structure of $\mathbf{T}$ to the dimensionality of the associated conductivity distribution. In particular, we note that for a two-dimensional (2-D) conductivity structure, there exists a real angle ψ_0 such that the rotated telluric transfer tensor $\mathbf{T}'(\psi)$ [cf. Eq. (4a)] assumes a diagonal form, viz.

$$\mathbf{T}'(\psi_0)=\begin{pmatrix}T'_{11}(\psi_0) & 0\\ 0 & T'_{22}(\psi_0)\end{pmatrix}. \tag{6}$$

In writing Eq. (6), we have implicitly assumed the parallelism of the sensor coordinate systems (1, 2) and (1′, 2′) for the base and satellite stations, respectively. Now, for 2-D geoelectric structures, the principal frame of reference (s, d) is defined to be that frame whose axes are aligned with the strike-dip directions for the structure (viz. with the principal structural axes). This principal frame can be obtained from the sensor coordinate frames (1, 2)≡(1′, 2′) by a pure rotation operation through some azimuthal angle $\psi=\psi_0$. Furthermore, for a true 2-D structure, the corresponding telluric transfer tensor is symmetric, so $T_{12}=T_{21}$. Continuing along this vein, it is straightforward to show from Eqs. (3) and (4) that for a telluric transfer tensor corresponding to some 2-D conductivity structure, the value of $\psi=\psi_0$ that results in the diagonal form of Eq. (6) is determined from

$$\tan 2\psi_0=T_1/T_3, \tag{7}$$

where T_1 and T_3 are defined as per Eq. (3b) and (3d). Although Eq. (7) permits the determination of the principal axes of the 2-D structure, there is still a $\pm\pi/2$ ambiguity in the identification of the strike and dip axes which can be resolved by a consideration of the magnetic transfer functions as will be shown later.

It should be noted that in the S-frequency interval, where the telluric fields essentially behave as DC fields, the elements of the telluric transfer tensor are real and independent of the frequency. In this particular frequency range, it is well known that for 2-D conductivity structure, the major and minor axes of the ellipse of polarization for the

output electric field vector phasor at the satellite station coincide with the principal structural axes (i.e. the strike-dip direction). In addition, the azimuth ψ_0 of the major axis of this polarization ellipse relative to the fixed measurement axis $1 \equiv 1'$ can be computed from the relation (Berdichevsky, 1960; Iliceto et al., 1986)

$$\tan \psi_0 = \frac{T_{11} T_{21} + T_{12} T_{22}}{T_{11}^2 + T_{12}^2 - g} = \frac{T_1}{T_3 + \sqrt{T_1^2 + T_3^2}}, \tag{8a}$$

where

$$g = L^2/2 - \sqrt{L^4/4 - J^2}, \tag{8b}$$

$$L^2 = T_{11}^2 + T_{12}^2 + T_{21}^2 + T_{22}^2, \tag{8c}$$

and

$$J = \det(\mathbf{T}) = T_{11} T_{22} - T_{12} T_{21}. \tag{8d}$$

It should perhaps be noted that Eq. (8a) provides the same principal frame of reference (s, d) for 2-D conductivity structures (i.e. the same longitudinal and transversal directions for the structure) as that determined from Eq. (7). Finally, we remark that for the telluric mapping method, the Jacobian J [cf. Eq. (8d)] has traditionally been the only parameter to be utilized in the interpretation of telluric anomalies, usually being displayed in the form of iso-J contour maps (Yungul, 1968). Recently, however, Iliceto and Santarato (1986) have used other parameters such as $|T'_{11}(\psi_0)|$, $\arg [T'_{11}(\psi_0)]$, etc.

Canonical decomposition of the telluric transfer tensor

The extraction of informative telluric parameters from the telluric transfer tensor can be solved systematically by the application of canonical decomposition to $\mathbf{T}$. This decomposition, which was originally developed for the analysis of the magnetotelluric (MT) impedance tensor (Yee, 1985; LaTorraca et al., 1986; Yee and Paulson, 1987), provides a structural representation for $\mathbf{T}$ in the sense that it explicitly exhibits the tensor in terms of eight physically relevant scalar parameters that are useful for the interpretation of telluric anomalies as well for the assessment of structural dimensionality. Canonical decomposition permits the logical definition of intrinsic or principal coordinate systems for both the input (base) and output (satellite) electric field spaces in a totally natural fashion without the need for any a priori information concerning the dimensionality of the geoelectric structure from which $\mathbf{T}$ was derived.

From a purely mathematical point of view, the canonical decomposition for $\mathbf{T}$ possesses exactly the same form as that for the MT impedance tensor. Indeed, since the transfer characteristics for the earth system coupling the base with the satellite stations are modelled as a two-input and two-output linear multichannel system with the transfer matrix $\mathbf{T} \in C^{2\times 2}$, the telluric transfer tensor thus admits to the decomposition (cf. Yee and Paulson, 1987)

$$\mathbf{T} = \mathbf{U} \boldsymbol{\Sigma} \mathbf{V}^{\dagger}, \tag{9a}$$

where

$$\boldsymbol{\Sigma} = \begin{pmatrix} \sigma_1 \exp(i\gamma_1) & 0 \\ 0 & \sigma_2 \exp(i\gamma_2) \end{pmatrix}, \tag{9b}$$

$$\mathbf{U} \equiv (|u_1\rangle |u_2\rangle) = \begin{pmatrix} \cos(\theta_s) & -\exp(-i\phi_s)\sin(\theta_s) \\ \exp(i\phi_s)\sin(\theta_s) & \cos(\theta_s) \end{pmatrix}, \tag{9c}$$

and

$$\mathbf{V} \equiv (|v_1\rangle |v_2\rangle) = \begin{pmatrix} \cos(\theta_b) & -\exp(-i\phi_b)\sin(\theta_b) \\ \exp(i\phi_b)\sin(\theta_b) & \cos(\theta_b) \end{pmatrix}. \tag{9d}$$

The parameters in this decomposition are constrained as follows: θ_s, $\theta_b \in [0, \pi/2]$; ϕ_s, $\phi_b \in (-\pi, \pi]$; γ_1, $\gamma_2 \in (-\pi, \pi]$; and $0 < \sigma_2 \leqq \sigma_1$. We emphasize that all these parameters are to be interpreted as functions of the frequency ω. It is possible to explicitly express the eight canonical parameters that emerge from this decomposition in terms of the elements of $\mathbf{T}$ as follows:

1) The singular values or principal telluric gains σ_1 and σ_2 of $\mathbf{T}$ can be computed from

$$\sigma_1^2 = \tfrac{1}{2} \|\mathbf{T}\|_F^2 + \{(\tfrac{1}{2} \|\mathbf{T}\|_F^2)^2 - |\det(\mathbf{T})|^2\}^{1/2} \tag{10a}$$

and

$$\sigma_2^2 = \tfrac{1}{2} \|\mathbf{T}\|_F^2 - \{(\tfrac{1}{2} \|\mathbf{T}\|_F^2)^2 - |\det(\mathbf{T})|^2\}^{1/2}, \tag{10b}$$

where

$$\begin{aligned} \|\mathbf{T}\|_F &= (|T_{11}|^2 + |T_{12}|^2 + |T_{21}|^2 + |T_{22}|^2)^{1/2} \\ &= [tr(\mathbf{T}^{\dagger}\mathbf{T})]^{1/2} \end{aligned} \tag{10c}$$

is the Frobenius norm of $\mathbf{T}$ and $\det(\mathbf{T})$ is the determinant of $\mathbf{T}$, represented by J in Eq. (8d).

2) The polarization parameters θ_b and ϕ_b which characterize the principal base (input) electric field polarization states are determined from

$$\tan(\theta_b) = \frac{|T_{11} T_{12}^* + T_{21} T_{22}^*|}{\sigma_1^2 - (|T_{12}|^2 + |T_{22}|^2)} \tag{11a}$$

and

$$\phi_b = \arg(T_{11} T_{12}^* + T_{21} T_{22}^*). \tag{11b}$$

3) Finally, the polarization parameters θ_s and ϕ_s which specify the principal satellite (output) electric field polarization states and the principal telluric phases γ_1 and γ_2 are given by

$$\tan(\theta_s) = \left| \frac{T_{21}\cos(\theta_b) + T_{22}\exp(i\phi_b)\sin(\theta_b)}{T_{11}\cos(\theta_b) + T_{12}\exp(i\phi_b)\sin(\theta_b)} \right|, \tag{12a}$$

$$\gamma_1 = \arg[T_{11}\cos(\theta_b) + T_{12}\exp(i\phi_b)\sin(\theta_b)], \tag{12b}$$

$$\phi_s = \arg[T_{21}\cos(\theta_b) + T_{22}\exp(i\phi_b)\sin(\theta_b)] - \gamma_1, \tag{12c}$$

and

$$\gamma_2 = \arg[T_{22}\cos(\theta_b) - T_{21}\exp(-i\phi_b)\sin(\theta_b)]. \tag{12d}$$

If the base electric field is measured with reference to the orthonormal (generally elliptic) basis states $|v_1\rangle$ and $|v_2\rangle$ [i.e. with reference to the principal base polarization states determined as per Eq. (9d)] so

$$|E^b_{v_1,v_2}\rangle = E^b_{v_1}|v_1\rangle + E^b_{v_2}|v_2\rangle = \begin{pmatrix} E^b_{v_1} \\ E^b_{v_2} \end{pmatrix}, \tag{13a}$$

and if the satellite electric field is measured with reference to the orthonormal (generally elliptic) basis states $|u_1\rangle$ and

$|u_2\rangle$ [i.e. with reference to the principal satellite polarization states determined as per Eq. (9c)] so

$$|E^s_{u_1,u_2}\rangle = E^s_{u_1}|u_1\rangle + E^s_{u_2}|u_2\rangle = \begin{pmatrix} E^s_{u_1} \\ E^s_{u_2} \end{pmatrix}, \tag{13b}$$

then the telluric transfer matrix referred to these input and output vector frames assumes the simple diagonal form

$$\mathbf{T}_P \equiv \mathbf{\Sigma} = \begin{pmatrix} \sigma_1 \exp(i\gamma_1) & 0 \\ 0 & \sigma_2 \exp(i\gamma_2) \end{pmatrix}, \tag{13c}$$

viz.

$$|E^s_{u_1,u_2}\rangle = \mathbf{T}_P |E^b_{u_1,u_2}\rangle. \tag{13d}$$

The diagonal elements of $\mathbf{T}_P$ determine the principal telluric transfer functions (i.e. principal complex transmittances between the base and satellite stations) for the earth system. In particular, the moduli (or principal gains) of these transfer functions (i.e. σ_1 and σ_2) correspond to the maximum and minimum electric field intensity transmittances between the base and satellite stations, where intensity transmittance is defined as the ratio of the output wave intensity (or power) to the input wave intensity, viz.

$$R \equiv \frac{\langle E^s|E^s\rangle}{\langle E^b|E^b\rangle} = \frac{\langle E^b|\mathbf{T}^\dagger\mathbf{T}|E^b\rangle}{\langle E^b|E^b\rangle}. \tag{14}$$

It is of interest to note that the input polarization states $|v_1\rangle$ and $|v_2\rangle$ (characterized by the polarization parameters θ_b and ϕ_b) which result in the maximum and minimum intensity (power) transmittances between the base and satellite stations, respectively, are orthogonal; and these input polarization states produce the output polarization states $|u_1\rangle$ and $|u_2\rangle$ (characterized by the polarization parameters θ_s and ϕ_s) which are also orthogonal.

We note that if the polarization form of an arbitrary polarization state

$$|p\rangle = \begin{pmatrix} p_1 \\ p_2 \end{pmatrix} = \begin{pmatrix} \cos(\theta) \\ \exp(i\phi)\sin(\theta) \end{pmatrix}$$

is characterized by the complex polarization ratio

$$P = p_2/p_1 = \tan(\theta)\exp(i\phi), \tag{15a}$$

then it is straightforward to show that the azimuth ψ [$\psi \in [0, \pi)$] and the ellipticity angle λ [$\lambda \in [-\pi/4, \pi/4]$] of the associated ellipse of polarizations is given by (Yee, 1985)

$$\tan 2\psi = \frac{2\,\mathrm{Re}(P)}{1-|P|^2} = \tan 2\theta \cos\phi \tag{15b}$$

and

$$\sin 2\lambda = \frac{2\,\mathrm{Im}(P)}{1+|P|^2} = \sin 2\theta \sin\phi. \tag{15c}$$

In terms of the elliptic parameters ψ and λ, the canonical decomposition for $\mathbf{T}$ displayed in Eq. (9a) may be expressed alternatively as

$$\mathbf{T} = \mathbf{R}(\psi_s)\,\mathbf{P}(\lambda_s)\,\bar{\mathbf{\Sigma}}\,\mathbf{P}(-\lambda_b)\,\mathbf{R}(-\psi_b), \tag{16a}$$

where

$$\bar{\mathbf{\Sigma}} = \begin{pmatrix} \sigma_1 \exp(i\bar{\gamma}_1) & 0 \\ 0 & \sigma_2 \exp(i\bar{\gamma}_2) \end{pmatrix} \tag{16b}$$

with

$$\bar{\gamma}_1 = \gamma_1 - (\xi_s - \xi_b), \tag{16c}$$

$$\bar{\gamma}_2 = \gamma_2 + (\xi_s - \xi_b), \tag{16d}$$

$$\xi_s = \arg(\cos\psi_s \cos\lambda_s - i \sin\psi_s \sin\lambda_s), \tag{16e}$$

and

$$\xi_b = \arg(\cos\psi_b \cos\lambda_b - i \sin\psi_b \sin\lambda_b). \tag{16f}$$

In Eq. (16a), $\mathbf{R}(\psi)$ and $\mathbf{P}(\lambda)$ are the rotation and ellipticity operators defined in Eqs. (4b) and (5b), respectively, and (ψ_s, λ_s) and (ψ_b, λ_b) are the elliptic parameters corresponding to the polarization parameters (θ_s, ϕ_s) and (θ_b, ϕ_b) computed in accordance with Eq. (15b) and (15c). Notice that, in general, both rotation and ellipticity transformations on $\mathbf{T}$ are required in order to obtain input and output coordinate frames in which the telluric transfer tensor assumes a simple diagonal form. It should be noted that polar diagrams of the elements of $\mathbf{T}$ are frequently constructed as a function of the azimuth (rotation) angle ψ to aid in the interpretation and classification of telluric anomalies. However, the canonical decomposition of $\mathbf{T}$ expressed in Eq. (16a) implies that in order to characterize optimally the dependence of the telluric anomalies on the polarization forms of the base (input) and satellite (output) electric fields, it is necessary also to construct polar diagrams for the elements of $\mathbf{T}$ as a function of the ellipticity angle λ. An examination of the polar diagrams as a function of both ψ and λ would enable the interpreter to specify the characteristic (optimal) polarizations at which the telluric anomalies are most revealing and distinctive. It is important to point out that the principal telluric gains σ_1 and σ_2 are independent of the polarization forms of the input and output electric fields and, consequently, these telluric parameters contain information pertaining solely to the intrinsic properties of the geoelectric structure.

For the most general 3-*D* conductivity structure, the eight canonical parameters σ_1, γ_1, σ_2, γ_2, θ_s, ϕ_s, θ_b and ϕ_b provide a complete specification of the telluric transfer tensor in terms of physically meaningful scalar parameters. These parameters can be used for the identification, discrimination and classification of the geometry and the nature of telluric anomalies. In particular, we note that for 2-D structures, the principal base and satellite basis states embodied in $\mathbf{V}$ and $\mathbf{U}$, respectively, are linearly polarized and aligned with each other; in particular, these principal basis states are linearly polarized along the strike and dip directions of the structure. This implies that $\theta_s = \theta_b$ and $\phi_s = \phi_b$ (i.e. the input and output principal states are aligned or parallel with each other) with $\phi_s = \phi_b = 0$ or π (i.e. the input and output principal states are linearly polarized). Hence, a 2-D structure is characterized by five canonical parameters, namely σ_1, γ_1, σ_2, γ_2 and $\theta_s = \theta_b \equiv \theta_0$. Note that $\psi_0 = \theta_0$ determines the angle through which the measurement (Cartesian) coordinate system (1, 2) $\equiv$ (1′, 2′) must be rotated in order to be aligned with the strike-dip (*s*, *d*) coordinate system. Of course, there still remains the problem of $a \pm \pi/2$ ambiguity in the determination or identification of the strike

and dip axes for the geoelectric structure. However, this ambiguity can be resolved if we have available additional information in the form of the magnetic parameters, as shown in the Appendix. In light of this discussion, it is important to emphasize that for 2-D conductivity structures, the canonical decomposition of **T** yields the same parameters as those extracted in the conventional analysis of **T** (Iliceto et al., 1986) based on the coordinate rotation properties of the tensor.

Furthermore, it is of interest to note that since the elements of **T** in the S-frequency interval associated with a 2-D structure are real with $T_{12}=T_{21}$, Eq. (11a) obtained from the canonical decomposition of **T** is identical to Eq. (8a) which was originally derived by Berdichevsky (1960) by an alternative method. In particular, to verify the equivalence between Eqs. (8a) and (11a), it is necessary to observe that [cf. Eq. (10a)–(10c)]

$$(|T_{11}|^2+|T_{12}|^2)-\sigma_2^2=\sigma_1^2-(|T_{21}|^2+|T_{22}|^2).$$

Finally, we note that canonical decomposition of the telluric transfer tensor for general 3-D conductivity structures provides eight scalar parameters that embody all the information contained in **T**. The parameters are more amenable to physical interpretation than any of the individual elements of **T** per se and, conceivably, they can be associated with certain features in the underlying conductivity structure. Indeed, since these canonical parameters embody information concerning the polarization transforming properties of the earth in its base and satellite electric field polarization states as well as information relating to the input-output behaviour (i.e. transfer characteristics) in its principal telluric transfer functions, they are diagnostic of the earth's subsurface conductivity distribution. Undoubtedly, the signatures provided by the canonical parameters can conceivably be employed to classify and characterize certain 3-D features in the conductivity distribution and, hence, may improve the interpretation of telluric data in the presence of 3-D distortions. However, before this can be done, it is necessary to undertake numerical and analog modelling as well as empirical studies of 3-D conductivity structures with the specific objective of studying how the behaviour of the canonical parameters is determined by the nature of the conductivity distribution. Hence, although the canonical decomposition of **T** provides a rigorous mathematical construct for studying the telluric tensor, modelling and empirical studies will be required in order to provide an understanding of the physical processes involved, particularly as it relates the nature of the conductivity distribution to their signatures as embodied in the canonical parameters. There is little doubt that such studies would significantly increase the potential of canonical decomposition as it relates to the inversion and interpretation of telluric data.

Separation of 2-D from 3-D structural components in T

Since the telluric mapping method has been primarily applied to the exploration of dipping sedimentary structures (i.e. geological structures which for the most part are characterized by geoelectric inhomogeneities that are elongated in some direction), the usual practice has been to interpret the telluric response in terms of 2-D conductivity models (Iliceto et al., 1986; Iliceto and Santarato, 1986). Indeed, the inversion and interpretation of telluric data have almost invariably been undertaken with reference to 2-D conductivity models since an extensive 3-D interpretation is usually deemed too computationally expensive and perhaps too extravagant given the quality and paucity of most data sets. In view of this, we will restrict our attention to telluric tensors that arise from comductivity structures that are dominated by a 2-D component on which is superimposed distortions or perturbations due to certain smaller 3-D contributions. Conventionally, the principal structural axes for quasi or near 2-D structures have been determined from the horizontal rotation properties of **T** with the assessment of the degree of influence from 3-D structural components being characterized in a somewhat semi-quantitative manner by the skewness parameter defined as

$$S=\frac{|T_{12}-T_{21}|}{|T_{11}+T_{22}|},$$

which provides an immediate assessment of the 3-D distortion of the purely 2-D situation. Of course, S vanishes for strictly 2-D structures. Accordingly, for quasi 2-D conductivity structures with S small (say, $S<0.20$), we remark that for the purpose of interpretation with 2-D forward modelling studies, it is perhaps more desirable to effect a separation of the 2-D and 3-D structural components from **T** and utilize only the 2-D component of the tensor in the construction of 2-D models.

Towards this primary objective, we consider the decomposition

$$\mathbf{T}=\mathbf{T}_A+\boldsymbol{\Delta}, \tag{17}$$

where $\mathbf{T}_A$ is that part of **T** due to the contribution from the strictly 2-D structural component and $\boldsymbol{\Delta}$ is that part of **T** arising from the 3-D geoelectric component. Of course, the latter contribution is viewed as a perturbation or noise in the ensuing analysis. If $\mathbf{T}_A$ is the result of a strictly 2-D geoelectric component, then, as already indicated in the previous section, its canonical parameters verify (1) $\theta_s^A=\theta_b^A$ and $\phi_s^A=\phi_b^A$ and (2) $\phi_s^A=\phi_b^A=0$ or π. Perhaps it should be noted that there exist certain 3-D conductivity structures (e.g. those which possess a vertical plane of mirror symmetry) whose telluric tensors result in canonical parameters that verify these two conditions, but we remark that this situation is rather exceptional and, consequently, conditions (1) and (2) can be considered to be necessary and sufficient conditions for two-dimensionality when taken from a purely practical or operational point of view. From this practical vantage point, we note that condition (1) implies that $\mathbf{T}_A$ commutes with its adjoint $\mathbf{T}_A^\dagger$ so $\mathbf{T}_A^\dagger\mathbf{T}_A=\mathbf{T}_A\mathbf{T}_A^\dagger$, viz. $\mathbf{T}_A$ is a normal matrix. This condition ensures that the principal input (base) and output (satellite) polarization states are aligned or parallel in the unitary (i.e. complex inner product) polarization space. We note that parallelism of polarization states in the unitary space requires the corresponding ellipses of polarization to possess identical azimuths and ellipticities. Furthermore, condition (2) implies that the input and output principal states are in fact linearly polarized so that the alignment (parallelism) between these states is actually maintained in real space. This development suggests that we can isolate the 2-D structural component from **T** (i.e. $\mathbf{T}_A$) using the following two-step procedure. Firstly, the normal matrix $\mathbf{T}_N$ that best approximates **T** is extracted and, secondly, the linear polariztion states that best approximate the input (or, equivalently, output) principal polariza-

tion states of this normal matrix are then obtained and used to construct $\mathbf{T}_A$.

To begin with, let us consider the problem of extracting the best normal matrix approximation for $\mathbf{T}$. To quantify 'best', we consider the matrix $\mathbf{T}_N$ that best approximates $\mathbf{T}$ to be the one that minimizes the 2-norm (Golub and Van Loan, 1983) of the perturbation matrix Δ, viz. $\mathbf{T}_N$ minimizes the cost function

$$\varepsilon \equiv \|\Delta\|_2 = \|\mathbf{T} - \bar{\mathbf{T}}_N\|_2 = \sigma_{\max}(\Delta), \tag{18}$$

where $\sigma_{\max}(\Delta)$ denotes the maximum singular value of Δ and $\bar{\mathbf{T}}_N$ is a member of the set consisting of all normal 2×2 matrices. A cautionary remark is in order here. This minimization problem does not possess a unique solution, and in the ensuing development we show how to construct one possible normal matrix which solves the problem.

The solution to the minimization problem can be obtained relatively easily from a purely geometric point of view. To this end, let us define the real and imaginary components of $\mathbf{T}$ as

$$\mathbf{T}_R = (\mathbf{T} + \mathbf{T}^\dagger)/2 \tag{19a}$$

and

$$\mathbf{T}_I = i(\mathbf{T} - \mathbf{T}^\dagger)/2, \tag{19b}$$

respectively. Notice that these two component operators are Hermitian and determine a Cartesian decomposition for $\mathbf{T}$ as $\mathbf{T} = \mathbf{T}_R + i\mathbf{T}_I$. Let $t_R^1 \geq t_R^2$ and $t_I^1 \geq t_I^2$ be the eigenvalues of $\mathbf{T}_R$ and $\mathbf{T}_I$, respectively, and observe that the normal matrix

$$\mathbf{T}_N^1 = \mathbf{T}_R + \frac{i}{2}(t_I^1 + t_I^2)\,\mathbf{I} \tag{20}$$

results in an error of approximation $\varepsilon_1 = (t_I^1 - t_I^2)/2$. This is easily verified by computing the perturbation matrix given by

$$\Delta^1 = i\mathbf{T}_I - \frac{i}{2}(t_I^1 + t_I^2)\,\mathbf{I}$$

and determining the maximum singular value. More importantly, the normal approximation of Eq. (20) can be endowed with a geometric interpretation as follows. As depicted in Fig. 2, the normal matrix given by Eq. (20) can be associated with a rectangle in the complex plane with corners determined by the points $t_R^1 + it_I^1$, $t_R^1 + it_I^2$, $t_R^2 + it_I^1$ and $t_R^2 + it_I^2$ which inscribe the ellipse $NR(\mathbf{T})$, where

$$NR(\mathbf{T}) \equiv \{\langle x|\mathbf{T}|x\rangle \in C : |x\rangle \in C^2, \langle x|x\rangle = 1\} \tag{21}$$

is the numerical range of $\mathbf{T}$ (Gantmacher, 1959; Donoghue, 1957). Observe that the sides of this rectangle are parallel to the real and imaginary axes, touching the ellipse at four tangential points of contact, and that the error of approximation in choosing the normal matrix of Eq. (20) is equal to one-half the length of the side of the rectangle parallel to the imaginary axis.

It is clear from Fig. 2 that the smallest error of approximation of $\mathbf{T}$ by a normal matrix is associated with that rectangle which inscribes $NR(\mathbf{T})$ and whose sides are parallel to the major and minor axes of the ellipse; and the error associated with this approximation is then equal to

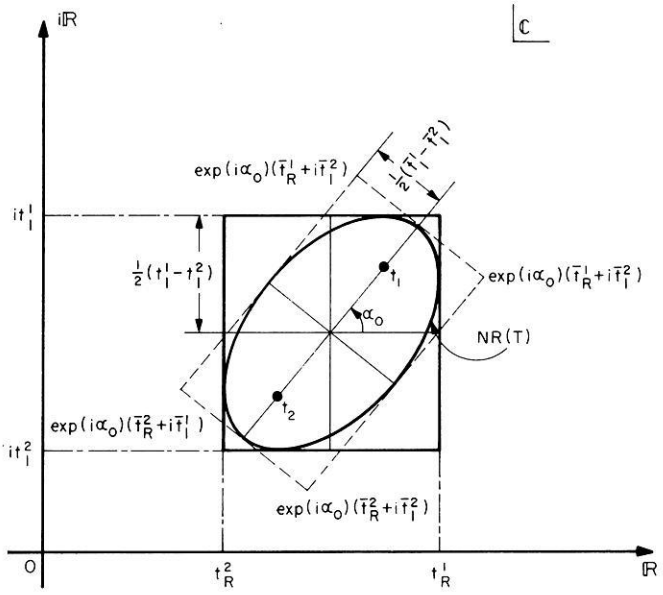

Fig. 2. Two rectangles that inscribe the ellipse corresponding to the numerical range of $\mathbf{T}$. These rectangles are associated with two possible normal matrix approximations for $\mathbf{T}$

one-half the length of the minor axis of the ellipse. This rectangle is delineated by dashed lines in Fig. 2. The normal approximation to $\mathbf{T}$ associated with the dashed rectangle is easily obtained by rotating $\mathbf{T}$ by an angle $-\alpha_0$ so that

$$\bar{\mathbf{T}} = \bar{\mathbf{T}}_R + i\bar{\mathbf{T}}_I \equiv \exp(-i\alpha_0)(\mathbf{T}_R + i\mathbf{T}_I), \tag{22a}$$

where

$$\bar{\mathbf{T}}_R = \mathbf{T}_R \cos\alpha_0 + \mathbf{T}_I \sin\alpha_0 \tag{22b}$$

and

$$\bar{\mathbf{T}}_I = -\mathbf{T}_R \sin\alpha_0 + \mathbf{T}_I \cos\alpha_0 \tag{22c}$$

are the real and imaginary components of $\bar{\mathbf{T}}$, respectively. The normal approximation of Eq. (20) is then applied to $\bar{\mathbf{T}}$ to form

$$\bar{\mathbf{T}}_N^1 = \bar{\mathbf{T}}_R + \frac{i}{2}(\bar{t}_I^1 + \bar{t}_I^2)\,\mathbf{I}, \tag{22d}$$

where $\bar{t}_I^1 \geq \bar{t}_I^2$ are the eigenvalues of $\bar{\mathbf{T}}_I$, and finally $\bar{\mathbf{T}}_N^1$ is rotated back by the angle α_0 with respect to the real axis in C to form the required optimal normal matrix approximation as

$$\mathbf{T}_N = \exp(i\alpha_0)\,\bar{\mathbf{T}}_N^1. \tag{22e}$$

Here α_0 denotes the angle that the major axis of the ellipse $NR(\mathbf{T})$ forms with the real axis. In light of the fact that eigenvalues t_1 and t_2 of $\mathbf{T}$ lie at the foci of $NR(\mathbf{T})$ (Donoghue, 1957), it is straightforward to compute explicitly this angle as

$$\alpha_0 = \arg(t_1 - t_2) = \arg\left(i\sqrt{\frac{\det(\mathbf{T}^-)}{|\det(\mathbf{T}^-)|}}\right), \tag{23a}$$

where

$$\mathbf{T}^- \equiv \mathbf{T} - \tfrac{1}{2}\,\mathrm{tr}(\mathbf{T})\,\mathbf{I}. \tag{23b}$$

Having obtained a required normal matrix $\mathbf{T}_N$ [cf. Eq. (22e)] that approximates $\mathbf{T}$ optimally, it remains to determine the linear polarization states that constitute the best approximation to the input (or, equivalently, output) principal polarization states of $\mathbf{T}_N$. If the canonical decomposition of $\mathbf{T}_N$ is written as

$$\mathbf{T}_N = \mathbf{U}_N \boldsymbol{\Sigma}_N \mathbf{U}_N^{\dagger}, \tag{24a}$$

where

$$\boldsymbol{\Sigma}_N = \begin{pmatrix} \sigma_1^N \exp(i\gamma_1^N) & 0 \\ 0 & \sigma_2^N \exp(i\gamma_2^N) \end{pmatrix} \tag{24b}$$

and

$$\mathbf{U}_N \equiv (|u_1^N\rangle |u_2^N\rangle) = \begin{pmatrix} \cos(\theta_N) & -\exp(i\phi_N)\sin(\theta_N) \\ \exp(i\phi_N)\sin(\theta_N) & \cos(\theta_N) \end{pmatrix}, \tag{24c}$$

then we are required to find

$$\mathbf{L}(\psi) \equiv (|l_1\rangle |l_2\rangle) = \begin{pmatrix} \cos\psi & -\sin\psi \\ \sin\psi & \cos\psi \end{pmatrix}, \tag{25}$$

such that the linear polarizations $|l_1\rangle$ and $|l_2\rangle$ are most closely aligned (parallel) to $|u_1^N\rangle$ and $|u_2^N\rangle$, respectively, in the unitary polarization space. To this end, let us first recall that the degree of alignment (parallelism) between two ket vectors $|x\rangle$ and $|y\rangle$ can be characterized by the angle χ between these vectors defined as

$$\cos\chi = |\langle x|y\rangle| / \sqrt{\langle x|x\rangle \langle y|y\rangle}.$$

In view of this, let us introduce the measure of alignment between the two pairs of polarization states $(|l_1\rangle, |u_1^N\rangle)$ and $(|l_2\rangle, |u_2^N\rangle)$ as

$$K = \frac{1}{2}\left\{ \frac{|\langle l_1|u_1^N\rangle|^2}{|\langle l_1|u_2^N\rangle|^2} + \frac{|\langle l_2|u_2^N\rangle|^2}{|\langle l_2|u_1^N\rangle|^2} \right\}. \tag{26}$$

Now, we need to compute the value of $\psi = \psi_0$ that maximizes K. Insertion from Eqs. (24c) and (25) of the definitions for $|l_k\rangle$ and $|u_k^N\rangle (k=1, 2)$ into Eq. (26) and evaluation of $dK/d\psi = 0$ leads to the result

$$\tan 2\psi_0 = \tan 2\theta_N \cos\phi_N. \tag{27}$$

Comparing Eq. (27) with Eq. (15b), we conclude that the linear polarization $|l_1\rangle$ that is maximally aligned with $|u_1^N\rangle$ in the unitary polarization space is oriented in real space in a direction parallel to the major axis of the ellipse of polarization of $|u_1^N\rangle$. Finally, the 2-D structural component of $\mathbf{T}$ is given by

$$\mathbf{T}_A = \mathbf{L}(\psi_0)\, \boldsymbol{\Sigma}_N\, \mathbf{L}^{\dagger}(\psi_0) \tag{28}$$

with $\boldsymbol{\Sigma}_N$ computed according to Eq. (24b) and ψ_0 determined as per Eq. (27).

Notice that the separation procedure developed above extracts the 2-D structural contribution from $\mathbf{T}$ at a single frequency. In some applications it may be desirable to generalize the procedure to extract the 2-D component that is applicable over a number of frequency points. In other words, we need to determine one regional principal coordinate system (characterized by the azimuthal elliptic parameter ψ_0) that is valid over some specified frequency range. It should be remarked that the azimuthal parameter ψ_0 is independent of frequency for true 2-D geoelectric structures. To develop a multi-frequency generalization of the separation procedure, we consider the maximization of the new cost function

$$K = \frac{1}{2}\left\{ \sum_{k=1}^{N} W_k \left[\frac{|\langle l_1|u_1^N(\omega_k)\rangle|^2}{|\langle l_1|u_2^N(\omega_k)\rangle|^2} + \frac{|\langle l_2|u_2^N(\omega_k)\rangle|^2}{|\langle l_2|u_1^N(\omega_k)\rangle|^2} \right] \right\}.$$

Here, $|u_1^N(\omega_k)\rangle$ and $|u_2^N(\omega_k)\rangle$ refer to the principal input and/or output polarization states extracted from the canonical decomposition of the normal approximation $\mathbf{T}_N(\omega_k)$ [cf. Eq. (27)] of $\mathbf{T}(\omega_k)$ at frequency $\omega_k (k=1, 2, \ldots, N)$. The scalars $W_k (k=1, 2, \ldots, N)$ are positive weights chosen a priori to pre-emphasize the telluric response at certain frequencies. Maximization of K with respect to ψ leads to the following expression for the orientation of the regional strike-dip structural axes with reference to the fixed measurement or sensor axes:

$$\tan 2\psi_0 = \frac{\sum_{k=1}^{N} W_k \sin[2\theta_N(\omega_k)] \cos[\phi_N(\omega_k)]}{\sum_{k=1}^{N} W_k \cos[2\theta_N(\omega_k)]}. \tag{29}$$

Observe that Eq. (29) is the multi-frequency generalization of Eq. (27).

A numerical example

Consider the ideal telluric transfer tensor

$$\mathbf{T}_{II} = \begin{pmatrix} 0.325 + 2.25i & -0.225\sqrt{3} - 0.7\sqrt{3}i \\ -0.225\sqrt{3} - 0.7\sqrt{3}i & 0.775 + 2.75i \end{pmatrix},$$

referred to Cartesian coordinate systems $(1, 2) \equiv (1', 2')$ rotated 30° ($\pi/6$ radians) with respect to the strike-dip coordinate system of some 2-D geoelectric structure. In particular, the principal telluric transfer functions are $T'_{11}(\pi/6) = 2.0025 \exp(i87.137°)$ and $T'_{22}(\pi/6) = 3.16228 \exp(i71.565°)$. Now suppose that the 2-D structure is contaminated and distorted by certain 3-D structural contributions and that the measured telluric tensor for the total contribution of 2-D and 3-D geoelectric components is given by

$$\mathbf{T} = \begin{pmatrix} 0.275 + 2.3i & -0.025\sqrt{3} - 0.5\sqrt{3}i \\ -0.425\sqrt{3} - 0.9\sqrt{3}i & 0.805 + 2.8i \end{pmatrix}.$$

First, we note that the skewness parameter for $\mathbf{T}$ has the value $S = 0.188$. For the purposes of comparison, we note that the application of a conventional rotation analysis of $\mathbf{T}$ [i.e. the determination of the rotation angle $\psi = \psi_0$ that minimizes the quantity $Q = |T'_{12}(\psi)|^2 + |T'_{21}(\psi)|^2$ in analogy to the equivalent condition utilized in magnetotelluric analysis (Vozoff, 1972)] yields a principal axis direction of $\psi_0 = 7.156°$. The principal telluric transfer functions can be obtained using Eq. (4) with $\psi = \psi_0$ and give $T'_{11}(\psi_0) = 2.635 \exp(i81.72°)$ and $T'_{22}(\psi_0) = 2.589 \exp(i74.30°)$.

Computation of the canonical decomposition of **T** results in the following values for the canonical parameters [cf. Eqs. (9)–(12)]: $\sigma_1 = 3.978$, $\gamma_1 = 82.105°$, $\sigma_2 = 1.323$, $\gamma_2 = 76.535°$, $\theta_s = 56.15°$, $\phi_s = 163.59°$, $\theta_b = 46.838°$ and $\phi_b = 172.27°$. Observe the 3-D structural contribution is expressed by the fact that the principal base and satellite polarization states are neither aligned (i.e. $\theta_s \neq \theta_b$ and $\phi_s \neq \phi_b$) nor linearly polarized (i.e. ϕ_s, $\phi_b \neq 0°$ or 180°).

Now, we proceed to apply the separation procedure described earlier to effect a separation of the 2-D and 3-D structural components from **T**. To this end, the real and imaginary components of **T** are

$$\mathbf{T}_R = \begin{pmatrix} 0.275 & -0.3897 + 0.3464i \\ -0.3897 - 0.3464i & 0.805 \end{pmatrix}$$

and

$$\mathbf{T}_I = \begin{pmatrix} 2.3 & -1.212 - 0.3464i \\ -1.212 + 0.3464i & 2.8 \end{pmatrix}$$

whose eigenvalues are $t_R^1 = 1.125$, $t_R^2 = -0.0449$ and $t_I^1 = 3.835$, $t_I^2 = 1.265$, respectively. Since the eigenvalues of **T** are $t_1 = 3.8512 \exp(i76.65°)$ and $t_2 = 1.3663 \exp(i82.0°)$, the major axis of the ellipse $NR(\mathbf{T})$ is oriented at $\alpha_0 = 73.708°$ [cf. Eq. (23a)] with reference to the real axis. Hence, the real and imaginary components of the rotated telluric tensor $\bar{\mathbf{T}} = \exp(-i\alpha_0)\,\mathbf{T}$ can be computed [cf. Eq. (22b) and (22c)] as

$$\bar{\mathbf{T}}_R = \begin{pmatrix} 2.285 & -1.273 - 0.2353i \\ -1.273 + 0.2353i & 2.913 \end{pmatrix}$$

and

$$\bar{\mathbf{T}}_I = \begin{pmatrix} 0.3813 & 0.03394 - 0.4297i \\ 0.03394 + 0.4297i & 0.0128 \end{pmatrix}$$

with eigenvalues given by $\bar{t}_R^1 = 3.931$, $\bar{t}_R^2 = 1.267$ and $\bar{t}_I^1 = 0.6658$, $\bar{t}_I^2 = 0.2717$, respectively.

With this information, the best normal matrix approximation can be computed and is found to be

$$\mathbf{T}_N = \begin{pmatrix} 0.4518 + 2.2483i & -0.1313 - 1.2880i \\ -0.5830 - 1.1559i & 0.6282 + 2.8517i \end{pmatrix}.$$

The canonical decomposition for $\mathbf{T}_N$ can now be computed to yield the following parameters [cf. Eq. (24)]: $\sigma_1^N = 3.936$, $\gamma_1^N = 76.58°$, $\sigma_2^N = 1.282$, $\gamma_2^N = 82.55°$, $\theta_N = 51.825°$ and $\phi_N = 169.53°$. The direction of the principal structural axes can be determined using Eq. (27) and is found to be $\psi_0 = 38.1°$. Note that this value for ψ_0 is closer to the true value of 30° than the one obtained using the conventional rotation analysis.

Conclusions

Canonical decomposition can be applied to the telluric transfer tensor to provide a complete set of eight physically motivated scalar parameters that can be used for the assessment of structural dimensionality as well as for the interpretation and classification of telluric anomalies. Indeed, canonical decomposition provides a rational basis for the interpretation of **T** by 3-D models since this analysis provides a complete specification of the tensor. Motivated by the form of the canonical decomposition for **T** arising from strictly 2-D geoelectric structures, we have developed a two-step procedure for the separation of 2-D from 3-D structural components in **T**. This is useful since, at present, only 2-D forward models are utilized in the interpretation of telluric data so that the separation procedure provides a means for the removal of distorting 3-D effects from the data prior to its submission to the interpretative phase.

Acknowledgements. This research was supported, in part, by grants provided by Saskatchewan Mining Development Corporation, University of Saskatchewan President's NSERC Fund and Energy, Mines and Resources, Canada (Research Agreement No. 86).

Appendix

Determination of strike and dip directions: a canonical decomposition approach

Canonical decomposition of the telluric transfer tensor permits the definition of a principal coordinate system for arbitrary geoelectric structures. However, for near 2-D structures, it is desirable to be able to identify the strike and dip directions for the structures. There still exists $a + \pi/2$ ambiguity in the determination of these structural axes from the principal coordinate system determined through canonical decomposition. This ambiguity can be resolved by making measurements of the three components of the total magnetic field at the base station. Choosing a right-handed Cartesian sensor coordinate system (x, y, z), the vertical component of the magnetic field can be expressed as the linear combination of the two horizontal components of the magnetic field, viz.

$$H_z = X_{zx} H_x + X_{zy} H_y \equiv \mathbf{X} |H\rangle, \tag{30}$$

where X_{zx} and X_{zy} are the magnetic parameters. In Eq. (30), $\mathbf{X} = (X_{zx}\ X_{zy})$ is the magnetic transfer matrix and $|H\rangle = (H_x, H_y)^T$ is the Cartesian tangential magnetic field vector phasor. Of course, if we assume that the source or primary field is a vertically incident plane electromagnetic wave, then the vertical component of the magnetic field at the surface of the earth is essentially a secondary or anomalous field whose magnitude comprises a measure of the degree of transversal inhomogeneity present in the underlying conductivity structure. It should perhaps be noted that this procedure for the identification of the strike direction, when used in conjunction with the telluric mapping method, involves additional measurements of the horizontal and vertical magnetic fields at the base station and, as such, can form the basis for the application of the more powerful telluric-magnetotelluric method (Hermance and Thayer, 1975). It is well known (Vozoff, 1972) that the direction of the horizontal magnetic field that possesses the largest correlation with H_z determines the direction of the dip axis of the geoelectric structure. This direction can be computed by application of the usual rotation analysis to **X** and yields the result

$$\tan 2\psi_d = \frac{2\,\mathrm{Re}(X_{zx}^* X_{zy})}{|X_{zx}|^2 - |X_{zy}|^2}, \tag{31}$$

where ψ_d is the angle that the dip axis makes with reference to the fixed x-measurement axis.

Since the magnetic transfer operator is a 1×2 complex matrix, we can compute the canonical decomposition for $\mathbf{X}$ as follows:

$$\mathbf{X} = \mathbf{U}_X \boldsymbol{\Sigma}_X \mathbf{V}_X^{\dagger}, \tag{32}$$

where

$$\boldsymbol{\Sigma}_X = \begin{pmatrix} \sigma_1^X \exp(i\gamma_1^X) & 0 \\ 0 & 0 \end{pmatrix}, \tag{33}$$

$$\mathbf{U}_X = 1, \tag{34}$$

and

$$\mathbf{V}_X \equiv (|v_1^X\rangle | v_2^X\rangle) = \begin{pmatrix} \cos(\theta_X) & -\exp(-i\phi_X)\sin(\theta_X) \\ \exp(i\phi_X)\sin(\theta_X) & \cos(\theta_X) \end{pmatrix}. \tag{35}$$

The canonical parameters σ_1^X, γ_1^X, θ_X and ϕ_X may be expressed explicitly in terms of the matrix elements of $\mathbf{X}$ to give

$$\sigma_1^X = (|X_{zx}|^2 + |X_{zy}|^2)^{1/2}, \tag{36}$$

$$\gamma_1^X = \arg(X_{zx}), \tag{37}$$

$$\cos(\theta_X) = \frac{|X_{zx}|}{\sqrt{|X_{zx}|^2 + |X_{zy}|^2}}, \tag{38}$$

and

$$\phi_X = \arg(X_{zx} X_{zy}^*) = \arg(X_{zx}) - \arg(X_{zy}). \tag{39}$$

We remark that for an input horizontal magnetic field polarized in the $|v_1^X\rangle$ direction in the unitary polarization space (i.e. $|H\rangle = |v_1^X\rangle$), the output vertical magnetic field H_z is equal to $\sigma_1^X \exp(i\gamma_1^X)$. In particular, σ_1^X is the maximum possible modulus of the output vertical magnetic field component for any input horizontal magnetic field $|H\rangle$ of unit wave intensity or power (i.e. $\langle H|H\rangle = 1$). It is of interest to note that σ_1^X coincides with the usual tipper magnitude (Vozoff, 1972) which has been utilized conventionally as an indicator of the significance of lateral conductivity inhomogeneities. Moreover, for an input horizontal magnetic field polarized in the $|v_2^X\rangle$ direction in the unitary polarization space, the output vertical magnetic field is completely extinguished; hence, $|v_2^X\rangle$ corresponds to an extinction or nulling direction for $\mathbf{X}$. Note that this direction is orthogonal to $|v_1^X\rangle$ in the unitary space. The direction of the dip axis can be obtained from the canonical parameters of $\mathbf{X}$ by use of Eqs. (15b), (38) and (39) to give

$$\tan 2\psi_d = \tan 2\theta_X \cos\phi_X = \frac{2|X_{zx}||X_{zy}|}{|X_{zx}|^2 - |X_{zy}|^2}\cos\phi_X = \frac{2\,\mathrm{Re}(X_{zx}^* X_{zy})}{|X_{zx}|^2 - |X_{zy}|^2}. \tag{40}$$

Observe that the dip axis direction derived from the canonical analysis of $\mathbf{X}$ is exactly the same as that obtained from the conventional rotation analysis [cf. Eqs. (31) and (40)]. Indeed, for a strictly 2-D geoelectric structure, the principal horizontal magnetic field polarization states are linearly polarized (i.e. $\phi_X = 0$) so that, for this case, Eq. (40) reduces down correctly to $\psi_d = \arctan(X_{zy}/X_{zx})$. It is of interest to remark that the canonical decomposition of $\mathbf{X}$ has systematically provided all the information from a purely mathematical point of view that the conventional examination (Vozoff, 1972) of $\mathbf{X}$ has revealed from a purely physical point of view.

For a geometric representation of the results embodied in the canonical decomposition of $\mathbf{X}$, it is convenient to introduce the induction arrow

$$\begin{aligned}\mathbf{N} &= \mathrm{Re}(\sigma_1^X \exp(i\gamma_1^X))\,\hat{\mathbf{r}}_1 + i\,\mathrm{Im}(\sigma_1^X \exp(i\gamma_1^X))\,\hat{\mathbf{r}}_2 \\ &= \sigma_1^X \cos\gamma_1^X\,\hat{\mathbf{r}}_1 + i\sigma_1^X \sin\gamma_1^X\,\hat{\mathbf{r}}_2,\end{aligned} \tag{41}$$

where $\hat{\mathbf{r}}_1$ and $\hat{\mathbf{r}}_2$ are unit vectors directed along the directions of the major and minor axes, respectively, of the ellipse of polarization associated with the principal input horizontal magnetic field polarization state $|v_1^X\rangle$ [cf. Eq. (35)]. It is of interest to note that the induction vector $\mathbf{N}$ is similar in structure to the Schmucker vector (Schmucker, 1970; Gregori and Lanzerotti, 1980). The real (in-phase) and imaginary (quadrature-phase) components of $\mathbf{N}$, namely

$$\mathrm{Re}(\mathbf{N}) = \sigma_1^X \cos\gamma_1^X\,\hat{\mathbf{r}}_1 \tag{42a}$$

and

$$\mathrm{Im}(\mathbf{N}) = \sigma_1^X \sin\gamma_1^X\,\hat{\mathbf{r}}_2, \tag{42b}$$

are aligned with the direction of the dip and strike axes, respectively, of the geoelectric structure. As with the Schmucker vector, the real induction arrow [i.e. Re(N)] always points away from regions or zones of higher electrical conductivity. Finally, notice that the magnitude of the induction vector $\mathbf{N}$ defined by

$$\|\mathbf{N}\| = \sqrt{\mathbf{N}\cdot\mathbf{N}^*} = \sqrt{\mathrm{Re}(\mathbf{N})\cdot\mathrm{Re}(\mathbf{N}) + \mathrm{Im}(\mathbf{N})\cdot\mathrm{Im}(\mathbf{N})} \tag{43}$$

is equal to σ_1^X, viz. $\|\mathbf{N}\|$ is simply the tipper magnitude.

References

Berdichevsky, M.N.: Electrical prospecting by the telluric current method. (in Russian) Moscow: Publishing House Gostoptekhizdat, 1960. English translation by G.V. Keller as Electrical prospecting with the telluric current method, Quarterly of the Colorado School of Mines, **60**(1), 1965

Donoghue, Jr., W.F.: On the numerical range of bounded operators. Mich. Math. J. **4**, 261–267, 1957

Gantmacher, F.R.: Theory of matrices. New York: Chelsea 1959

Golub, G.H., Van Loan, C.F.: Matrix computations. Baltimore: The John Hopkins University Press 1983

Gregori, G.P., Lanzerotti, L.J.: Geomagnetic depth sounding by induction arrow representation: a review. Rev. Geophys. Space Phys. **18**, 203–209, 1980

Hermance, J.F., Thayer, R.E.: The telluric-magnetotelluric method. Geophysics **40**, 664–668, 1975

Iliceto, V., Santarato, G.: On the possibility of the telluric method: some results on faulted structures. Geophys. Prosp. **34**, 1082–1098, 1986

Iliceto, V., Malaguti, R., Santarato, G.: A model study of telluric fields in two-dimensional structures. Geophys. J. R. Astron. Soc. **86**, 399–412, 1986

LaTorraca, G.A., Madden, T.R., Korringa, J.: An analysis of the magnetotelluric inpedance for three-dimensional conductivity structures. Geophysics **51**, 1819–1829, 1986

Schmucker, U.: Anomalies of geomagnetic variations in the southwestern United States. Bull. Scripps Inst. Oceanogr., Monograph **13**, 1970

Vozoff, K.: The magnetotelluric method in the exploration of sedimentary basins. Geophysics **37**, 98–141, 1972
Yee, E.: The magnetotelluric impedance tensor – its reconstruction and analysis. Ph.D. Thesis, Department of Physics, University of Saskatchewan, Saskatoon, 1985
Yee, E., Paulson, K.V.: The canonical decomposition and its relationship to other forms of magnetotelluric impedance tensor analysis. J. Geophys. **61**:173–189, 1987
Yungul, S.H.: Telluric sounding – a magnetotelluric method without magnetic measurements. Geophysics **31**, 185–191, 1966
Yungul, S.H.: Measurements of telluric "relative ellipse area" by means of "vectograms". Geophysics **33**, 127–131, 1968

Received December 18, 1986; revised May 21, 1987
Accepted July 1987